

## Supplementary Materials for

### **Electrokinetic Janus micromotors moving on topographically flat chemical patterns**

Tao Huang<sup>1,2</sup>, Vyacheslav Misko<sup>3,4</sup>, Anja Caspari<sup>5</sup>, Alla Synytska<sup>5,6,7</sup>, Bergoi Ibarlucea<sup>2</sup>, Franco Nori<sup>4,8</sup>, Jürgen Fassbender<sup>9</sup>, Gianauelio Cuniberti<sup>2</sup>, Denys Makarov<sup>9</sup>, Larysa Baraban<sup>1\*</sup>

<sup>1</sup>Helmholtz-Zentrum Dresden-Rossendorf e.V., Institute of Radiopharmaceutical Cancer Research, Bautzner Landstrasse 400, 01328 Dresden, Germany

<sup>2</sup>Max Bergmann Center of Biomaterials and Institute for Materials Science, Technische Universität Dresden, 01062 Dresden, Germany

<sup>3</sup>μFlow group, Department of Bioengineering Sciences, Department of Chemical Engineering, Vrije Universiteit Brussel, Pleinlaan 2, 1050 Brussels, Belgium

<sup>4</sup>Theoretical Quantum Physics Laboratory, RIKEN Cluster for Pioneering Research, Wako-shi, Saitama 351-0198, Japan

<sup>5</sup>Leibniz-Institut für Polymerforschung Dresden e.V., Hohe Straße 6, 01069, Dresden, Germany.

<sup>6</sup>Institute of Physical Chemistry and Polymer Physics, Technische Universität Dresden, 01062 Dresden, Germany

<sup>7</sup>Bavarian Polymer Institute (BPI), University of Bayreuth, Universitätsstraße 30, 95447 Bayreuth, Germany

<sup>8</sup>Physics Department, University of Michigan, Ann Arbor, Michigan 48109-1040, USA.

<sup>9</sup>Helmholtz-Zentrum Dresden-Rossendorf e.V., Institute of Ion Beam Physics and Materials Research, Bautzner Landstrasse 400, 01328 Dresden, Germany

Corresponding author: [l.baraban@hzdr.de](mailto:l.baraban@hzdr.de)

ORCID: 0000-0003-1010-2791

## Supplementary Note 1

COMSOL simulations are based on the model developed by Wang et al.<sup>1</sup> and Velegol<sup>2</sup>. In this model, AgCl caps on Janus particles decompose under blue light illumination and release Cl<sup>-</sup> ions and H<sup>+</sup> ions. The local electric ( $E$ ) field is generated by the different diffusivities of H<sup>+</sup> and Cl<sup>-</sup> ions. The electroosmotic flow is induced by this local  $E$ -field.

The simulations are performed by using electrostatics and creeping flow modules of COMSOL Multiphysics. The simulation is built by placing Janus particles on a charged pattern substrate (containing regions with different Zeta potential  $\zeta_{APTES}$  and  $\zeta_{GOLD}$ ), which is immersed in the center of the simulation domain in form of a square with side length of 100  $\mu\text{m}$ . The particle-to-substrate separation distance is set 1  $\mu\text{m}$ . The Janus particle is shown by a circle of 2  $\mu\text{m}$  in diameter (Supplementary Figure 4), with equal half-circles representing two hemispheres: PS (right half-circle) and AgCl (left). The Janus particle is fixed, and the fluid is allowed to flow freely around the Janus particle.

In simulation, the AgCl decomposition reaction is presented in a simplified manner as the flux of H<sup>+</sup> and Cl<sup>-</sup> ions release from the AgCl hemisphere. The flux of the released ions ( $J$ ) and the diffusion coefficients ( $D$ ) of H<sup>+</sup> and Cl<sup>-</sup> ions are:  $J = 1.6 \times 10^{-5} \text{ mol m}^{-2} \text{ s}^{-1}$ ,  $D_{H^+} = 9.311 \times 10^{-9} \text{ m}^2 \text{ s}^{-1}$ ,  $D_{Cl^-} = 2.031 \times 10^{-9} \text{ m}^2 \text{ s}^{-1}$ , respectively.<sup>1</sup> The Zeta potential of the Janus particle is measured to be +27 mV, and the Zeta potential of the APTES and gold layers are  $\zeta_{APTES} = 14.5 \text{ mV}$ ,  $\zeta_{GOLD} = -45.8 \text{ mV}$ , respectively.

In the Electrostatic module, the initial value of the electric potential of the medium is set to be 0 V. The four outside boundaries are held at 0 potential. The space charge density, which determines the potential and electric field distribution, is set as a variable under "Definition" in the model. In addition to its intrinsic Zeta potential, the AgCl half-circle carries an extrinsic surface charge density  $\rho_s$  originating from the surface reaction and related to the flux of ions  $J$  and the diffusivities of H<sup>+</sup> and Cl<sup>-</sup>:

$$\rho_s = \varepsilon E = \varepsilon \frac{J k_B T}{2 e n_0} \left( \frac{1}{D_{H^+}} - \frac{1}{D_{Cl^-}} \right) \quad (1)$$

where  $\varepsilon$  is the medium electrical permittivity,  $E$  is the electric field,  $J$  is the flux of the released ions,  $e$  is the proton charge,  $n_0$  is the initial ion concentration of the water,  $k_B$  is the Boltzmann constant,  $T$  is the temperature,  $D_{H^+}$  and  $D_{Cl^-}$  are diffusion coefficients of  $H^+$  and  $Cl^-$  ions.

On the PS side of the Janus particle, we set:  $\rho_s = 0$ .

In the creeping flow module, the fluid was set as incompressible, inertia was neglected to simulate the Stokes flow condition. The boundary conditions for left and right side walls are set to be open boundaries and the bottom and top sides are set as slip boundaries (Supplementary Figure 4). The Janus particle surface is set as no-slip boundary. The charged pattern substrate is set as electroosmotic velocity. The electric field is solved by Electrostatic module and the tangential electric field is used in the electroosmotic velocity boundary condition. The zeta potential of charged pattern surface (gold and APTES functionalized) is used for COMSOL to calculate the electroosmotic mobility. The creeping flow module is used to calculate fluid flows outside the electrical double layers (EDL), which are governed by the Stokes flow:  $\eta \nabla^2 u = 0$  and  $\nabla \cdot u = 0$ , where  $\eta$  is the dynamic viscosity of the solution and  $u$  is the fluid speed, with the assumption of infinitesimal EDL. Outside the EDL, the electrostatic potential  $V$  is found by solving the Laplace equation,  $\nabla^2 V = 0$ . The electrostatics module is used to calculate the electric field distribution in space with following equation:

$$E = -\nabla V \quad (2)$$

The space charge density is used to calculate the local electric field,  $E$ , accord to the following equation:

$$\nabla(\varepsilon E) = \rho_v \quad (3)$$

where  $\varepsilon$  is the medium electrical permittivity,  $\rho_v$  is the space charge density.

The creeping flow module and electrostatics module are coupled by an electroosmotic boundary condition. On the surface with a charged pattern, the flow boundary condition is governed by an electroosmotic slip velocity:

$$\mathbf{U}_{eo} = \frac{\zeta \varepsilon \mathbf{E}_t}{\eta} \quad (4)$$

where  $\mathbf{E}_t$  is the tangential component of the local electric field.  $\zeta$  is the zeta potential of the charged pattern surface.

Meshing is done by setting user-controlled mesh conditions. The element size is set to be extremely fine. Boundary layers can be used to create meshes for the Janus particle and charged pattern surface. Free triangular mesh is used for all the meshing operations.

In this model, Janus particle is fixed, and the fluid is allowed to flow freely. The Janus particle surface is set as no-slip boundary. The charged pattern substrate is set as electroosmotic velocity. We only model the electroosmotic flow on the APTES/Gold charged pattern. The average electroosmotic flow velocity  $\overline{U}_{eo}$  magnitude under the Janus particle calculates by:

$$\overline{U}_{eo} = \frac{\int_a^b \mathbf{U}_{eo} dL}{\int_a^b dL} \quad (5)$$

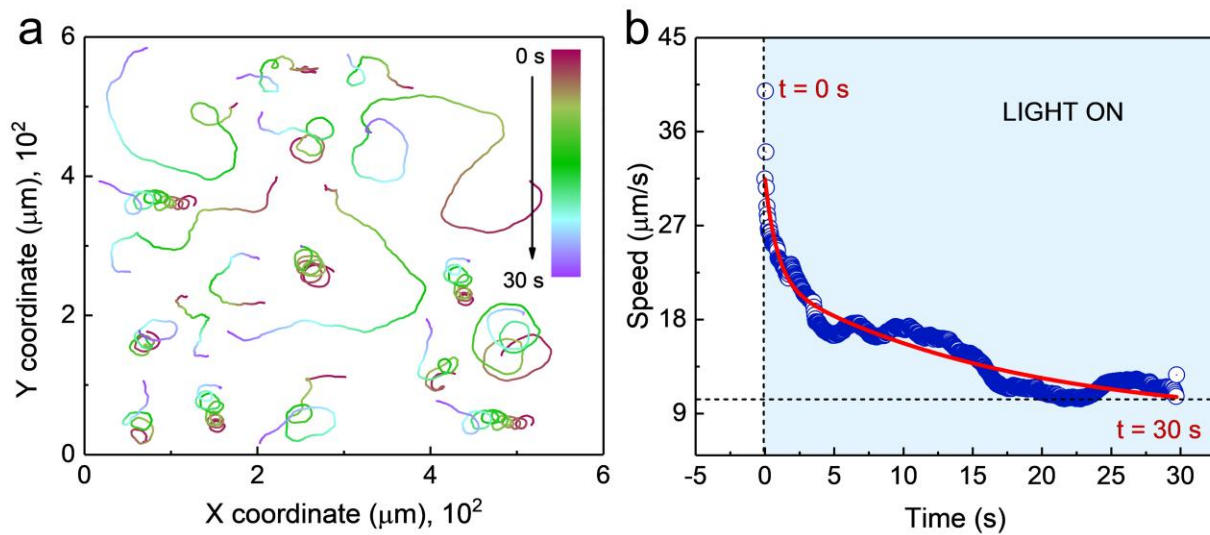
Where  $L$  is the distance from point a to point b (Supplementary Figure 5).

**Supplementary Table 1. Parameters for COMSOL models.**

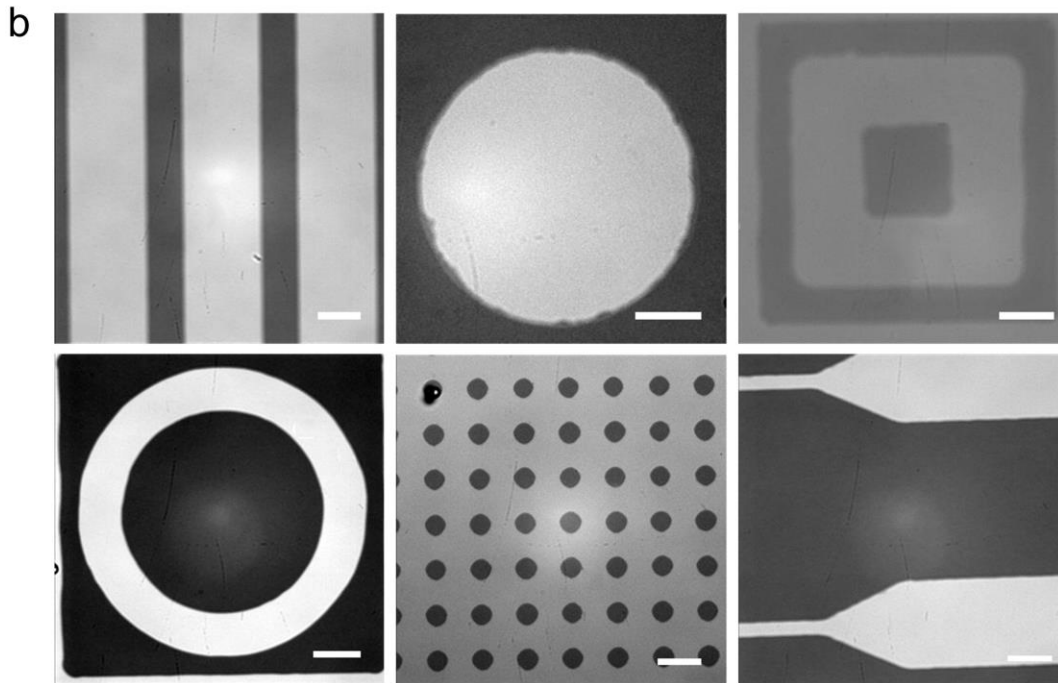
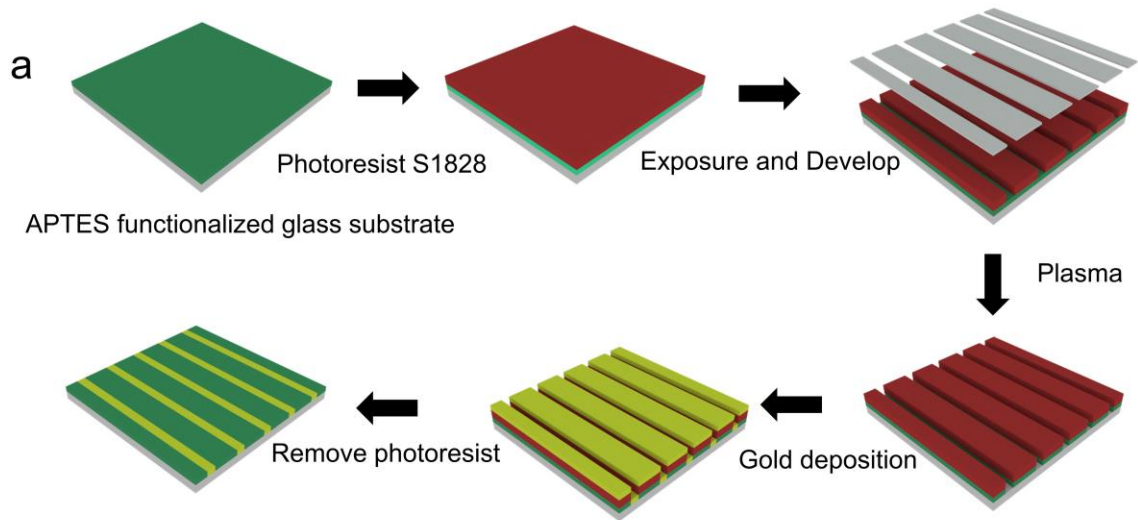
	Value	Description
Flux <sub>Cl<sup>-</sup></sub>	$1.6 \times 10^{-5} \text{ mol m}^{-2} \text{ s}^{-1}$	Cl <sup>-</sup> release flux
Flux <sub>H<sup>+</sup></sub>	$1.6 \times 10^{-5} \text{ mol m}^{-2} \text{ s}^{-1}$	H <sup>+</sup> release flux
Zeta <sub>Gold</sub>	-0.0458 V	Zeta potential of gold substrate
Zeta <sub>APTES</sub>	0.145 V	Zeta potential of APTES substrate
D <sub>H<sup>+</sup></sub>	$9.331 \times 10^{-9} \text{ m}^2 \text{ s}^{-1}$	Diffusion coefficient of H <sup>+</sup>
D <sub>Cl<sup>-</sup></sub>	$2.031 \times 10^{-9} \text{ m}^2 \text{ s}^{-1}$	Diffusion coefficient of Cl <sup>-</sup>
T	293.15K	
e	$1.602176634 \times 10^{-19} \text{ C}$	proton charge
n <sub>0</sub>	$2.24 \times 10^{-3} \text{ mol m}^{-3}$	Initial ion concentration of the water
Vacuum permittivity	$8.854187817 \times 10^{-12} \text{ F m}^{-1}$	
Relative permittivity of water	80	
k <sub>B</sub>	$1.38064852 \times 10^{-23} \text{ m}^2 \text{ kg s}^{-2} \text{ K}^{-1}$	Boltzmann constant

**Supplementary Table 2. Variables for COMSOL models.**

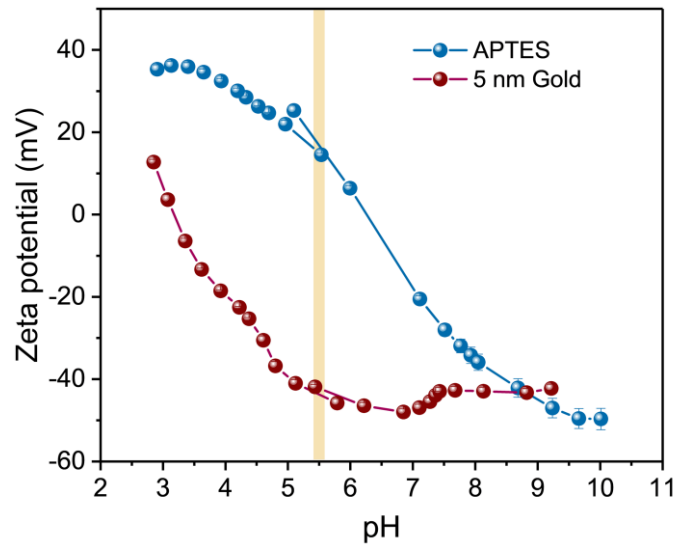
	Value	Description
ρ <sub>s</sub>	$\rho_s = \varepsilon E = \varepsilon \frac{jk_B T}{2en_0} \left( \frac{1}{D_{H^+}} - \frac{1}{D_{Cl^-}} \right)$	Space charge density



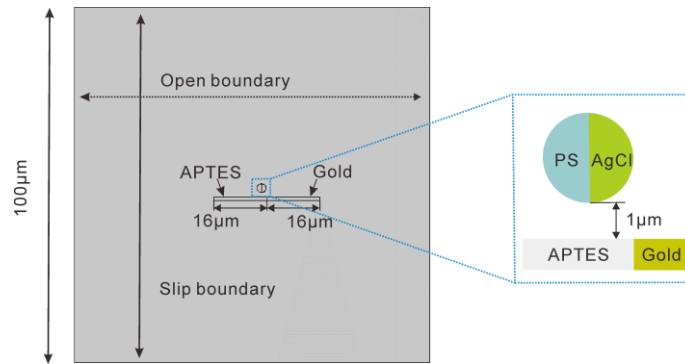
**Supplementary Figure 1. Trajectories and speed analysis of Janus particles under blue light illumination.** (a) Trajectories of 20 single PS/Ag/AgCl/ $\beta$ -FeOOH Janus micromotors taken over 30 s under blue light illumination. (b) Experimentally measured the time evolution of the speed of Janus micromotor. Red solid line as a guide to the eye.



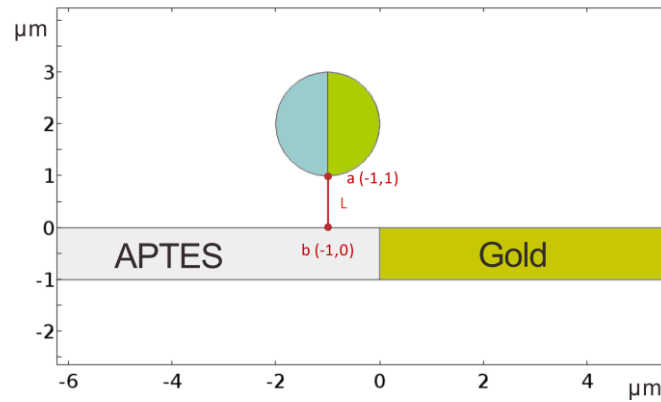
**Supplementary Figure 2. Charged pattern preparation.** (a) Schematic representation of the lithographic patterning of the sample to create the charged patterns for particle guidance. (b) Optical micrograph of APTES/Gold charged pattern. Different geometries are shown including straight stripe pattern, circular pattern, square ring, circle ring, circular dots array, and flow-focusing structures. Scale bar: 10  $\mu\text{m}$ .



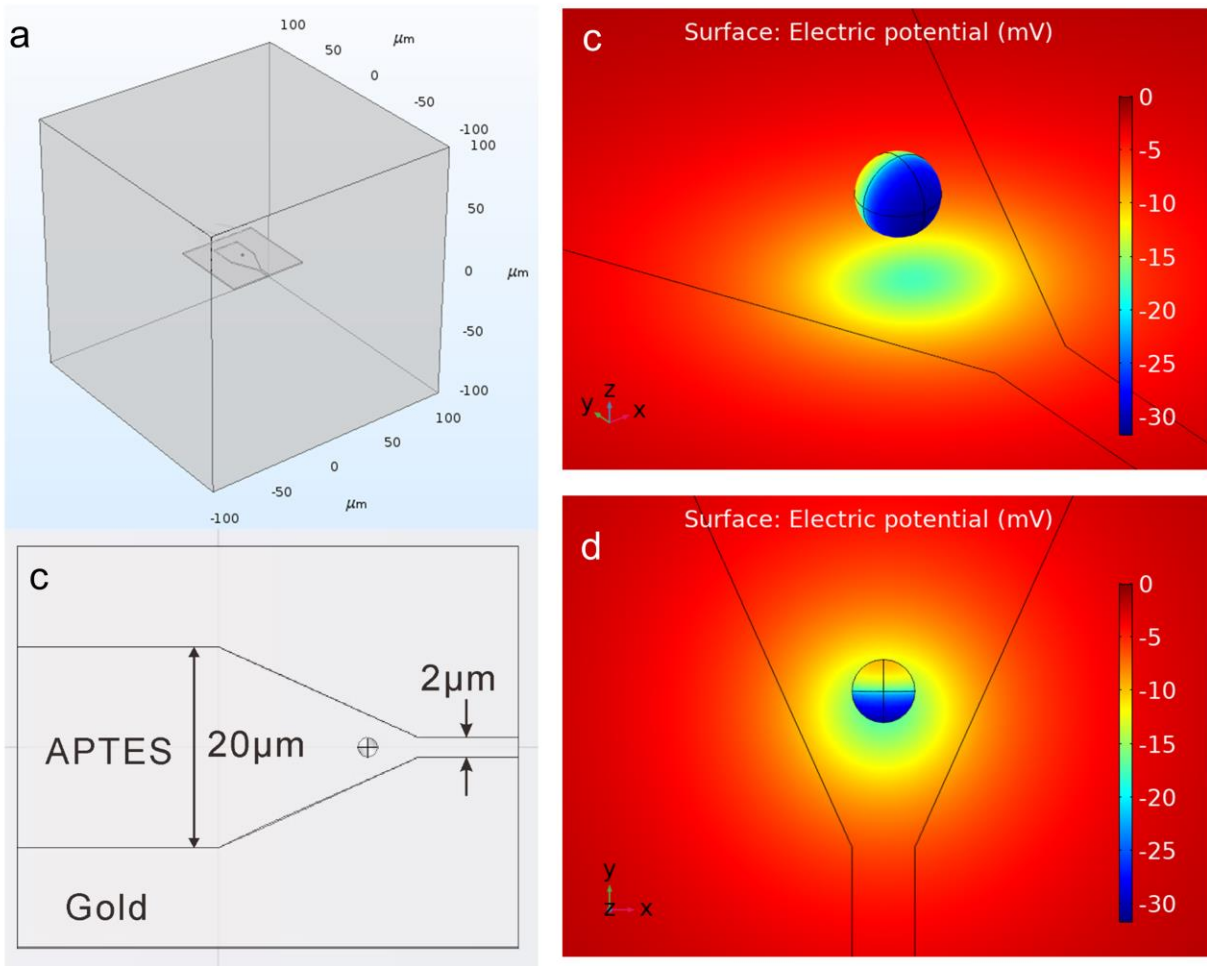
**Supplementary Figure 3. Zeta potential vs. pH on the APTES-modified glass substrate and gold-coated substrate.** The thickness of the Au layer is 5 nm. The thickness of the APTES coating is 4 nm. Yellow shade corresponds to the pH ranges of the experiments. Error bars indicate the standard deviations of the average values of Zeta potential.



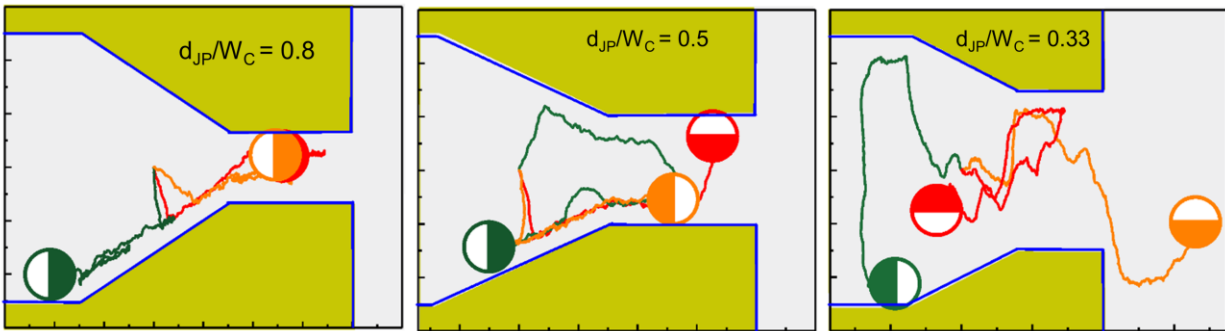
**Supplementary Figure 4. 2D geometry (side view) of a Janus sphere used in COMSOL simulations.** The Janus particle is positioned 1  $\mu\text{m}$  above the surface.



**Supplementary Figure 5. The averaged electroosmotic flow velocity magnitude under the Janus particle calculates by line averaged from point a to point b.**



**Supplementary Figure 6. 3D COMSOL simulation results when Janus particles move in a flow-focusing charged pattern.** (a) A 3D space used for calculations. (b) Dimensions of the flow-focusing geometry. A sphere of  $2\mu\text{m}$  in diameter is indicated in (b) with a circle with a cross. The sphere is placed above a charged surface with a separation distance of  $1\mu\text{m}$ . The charged pattern and the Janus particle are placed in the center of a cube with a side length of  $200\mu\text{m}$  (panel (a)). (c, d) The distribution of the electric potential around a Janus particle. The color code indicates the magnitude of electric potential.



**Supplementary Figure 7. Molecular-dynamics simulations of the trajectories of Janus particles in the constriction of various ratios  $d_{JP}/W_C$ : 0.8, 0.5 and 0.33.** Possible scenarios: Janus particles moving back to the wide channel from the initial position moving towards the constriction and reflecting, entering the constriction and then turning back, and passing the constriction. Green trajectory illustrates the scenario: when a particle moves back to the wide channel. The red trajectory shows when a particle enters the constriction but later turns back. The orange trajectory shows when a Janus particle passes all the way through the constriction.

**Supplementary Table 3. Statistical analysis of the Janus micromotor moving behavior at the APTES/gold interface.** At the APTES/gold interface, three types of moving behavior were observed. The Janus micromotor shows two-dimensional (2D) rotation of the cap (2D reflection), three-dimensional (3D) rotation of the cap (3D reflection), or just crosses the interface. in the case of 2D and 3D reflection, the incident angle is always smaller than the reflection angle. Then, the proportion of each scenario was assessed.

	<b>Incident angle</b> <b>(<math>\theta_1</math>)</b>	<b>Reflection angle</b> <b>(<math>\theta_2</math>)</b>	<b>Behavior</b>	<b>Percentage</b>
Video 1	41°	83°		
Video 2	14°	69°		
Video 3	29°	84°		
Video 4	31°	77°	2D reflection	66.7%
Video 5	25°	83°		
Video 6	53°	74°		
Video 7	25°	74°		
Video 8	26°	78°		
Video 9	9°	21°	3D reflection	16.7%
Video 10	5°	24°		
Video 11	9°	---	Cross	16.7%
Video 12	6°	---		

## Supplementary References

- 1 Zhou, C., Zhang, H. P., Tang, J. Y. & Wang, W. Photochemically Powered AgCl Janus Micromotors as a Model System to Understand Ionic Self-Diffusiophoresis. *Langmuir* **34**, 3289-3295, doi:10.1021/acs.langmuir.7b04301 (2018).
- 2 Kline, T. R. *et al.* Catalytically driven colloidal patterning and transport. *J. Phys. Chem. B* **110**, 24513-24521 (2006).